Lung Ultrasound for Critically Ill Patients

Francesco Mojoli[1,2], Bélaid Bouhemad[3,4], Silvia Mongodi[2], and Daniel Lichtenstein[5]

[1]Department of Clinical-Surgical, Diagnostic, and Pediatric Sciences, Unit of Anaesthesia and Intensive Care, University of Pavia, Pavia, Italy; [2]Anestesia e Rianimazione I, Fondazione Istituto di Ricovero e Cura a Carattere Scientifico, Policlinico San Matteo, Pavia, Italy; [3]Dijon et Université Bourgogne Franche-Comté, Lipides Nutrition Cancer Unité Mixte de Recherche 866, Dijon, France; [4]Département d'Anesthésie et Réanimation, Centre Hospitalier Universitaire Dijon, Dijon, France; and [5]Medical Intensive Care Unit, Hospital Ambroise Paré, Boulogne (Paris-West University), France

ORCID ID: 0000-0002-6031-6336 (F.M.).

Abstract

Point-of-care ultrasound is increasingly used at the bedside to integrate the clinical assessment of the critically ill; in particular, lung ultrasound has greatly developed in the last decade. This review describes basic lung ultrasound signs and focuses on their applications in critical care. Lung semiotics are composed of artifacts (derived by air/tissue interface) and real images (i.e., effusions and consolidations), both providing significant information to identify the main acute respiratory disorders. Lung ultrasound signs, either alone or combined with other point-of-care ultrasound techniques, are helpful in the diagnostic approach to patients with acute respiratory failure, circulatory shock, or cardiac arrest. Moreover, a semiquantification of lung aeration can be performed at the bedside and used in mechanically ventilated patients to guide positive end-expiratory pressure setting, assess the efficacy of treatments, monitor the evolution of the respiratory disorder, and help the weaning process. Finally, lung ultrasound can be used for early detection and management of respiratory complications under mechanical ventilation, such as pneumothorax, ventilator-associated pneumonia, atelectasis, and pleural effusions. Lung ultrasound is a useful diagnostic and monitoring tool that might in the near future become part of the basic knowledge of physicians caring for the critically ill patient.

Keywords: thoracic ultrasound; mechanical ventilation; lung monitoring; acute respiratory failure

In recent years, ultrasound has earned a leading position among imaging techniques integrating clinical and instrumental bedside assessment of the critically ill (1). Point-of-care ultrasound is now generally recognized as useful and in some cases mandatory—for instance, for procedure guidance (2). Its application at the bedside includes differential diagnosis and therapeutic management of complex clinical pictures, such as hemodynamic instability (3), acute respiratory failure (4), or cardiac arrest (5). Multiple ultrasound techniques are here combined, and among these, lung ultrasound has developed the most in the last few years.

Although the first description of ultrasound evaluation of the lung dates back 50 years ago (6), and basic signs in lung ultrasound were systematically described in the 1990s (7–10), the technique has spread mainly in the last decade, and its positive impact on clinical management is now suggested (11, 12). This review describes basic lung ultrasound semiotics and its applications in the critically ill, with specific focus on the mechanically ventilated patient.

The Technique and Basic Semiotics

In the thorax, air and water mingle: this explains the signs of lung ultrasound (8). Because of the difference in acoustic impedance between air in the lung and superficial tissues, ultrasound cannot penetrate the lung, and artifacts are generated by the pleura. A peculiarity of lung ultrasound findings is that they are made up of both artifacts (normal and pathological) and real images (always pathological and visible only in the absence of air interposition).

(Received in original form February 5, 2018; accepted in final form October 24, 2018)

Author Contributions: All authors made substantial contribution to the conception and design of the work; all authors drafted the work and revised it critically before submission (introduction: F.M., B.B., S.M., and D.L.; technique and basic semiotics: F.M., B.B., S.M., and D.L.; a diagnostic tool for the acute patient: F.M., B.B., S.M., and D.L.; a monitoring tool: F.M., B.B., and S.M.; lung ultrasound–guided mechanical ventilation: F.M., B.B., and S.M.; detection and management of respiratory complications: F.M., B.B., and S.M.; limitations: F.M., B.B., S.M., and D.L.; conclusions: F.M., B.B., S.M., and D.L.; tables and figures: F.M., B.B., S.M., and D.L.).

Correspondence and requests for reprints should be addressed to Francesco Mojoli, M.D., Rianimazione I, Fondazione IRCCS Policlinico S. Matteo, Viale Golgi 19, Pavia, Italy. E-mail: francesco.mojoli@unipv.it.

This article has an online supplement, which is accessible from this issue's table of contents at www.atsjournals.org.

CME will be available for this article at www.atsjournals.org.

Am J Respir Crit Care Med Vol 199, Iss 6, pp 701–714, Mar 15, 2019
Copyright © 2019 by the American Thoracic Society
Originally Published in Press as DOI: 10.1164/rccm.201802-0236CI on October 29, 2018
Internet address: www.atsjournals.org

Here, we schematically recall the basic principles of lung ultrasound, its main signs, and how they are generated; the definitions we use correspond to the 2012 international consensus conference (13) (Figures 1–3 and Table 1). A simple machine is perfectly suitable; in modern machines, harmonics and artifact-erasing software have to be deactivated. There is no evidence of any one probe being better than another: a single high-resolution microconvex probe with wide frequency range or a combination of a linear high-frequency probe and a convex/phased-array low-frequency probe can be used; high- and low-frequency settings adequately assess both the pleura and deeper findings, such as consolidations and effusions.

The lung is a broad organ and many standardizations have been proposed for exploring it. The Bedside Lung Ultrasound in Emergency (BLUE) protocol defines three points of interest per lung, the "BLUE-points" (4). The international consensus conference (13) suggests an eight-region approach for anterolateral field examination in the emergency department, whereas a more comprehensive twelve-region examination is frequently used in the ICU (*see* Figure E1 in the online supplement) (14–16).

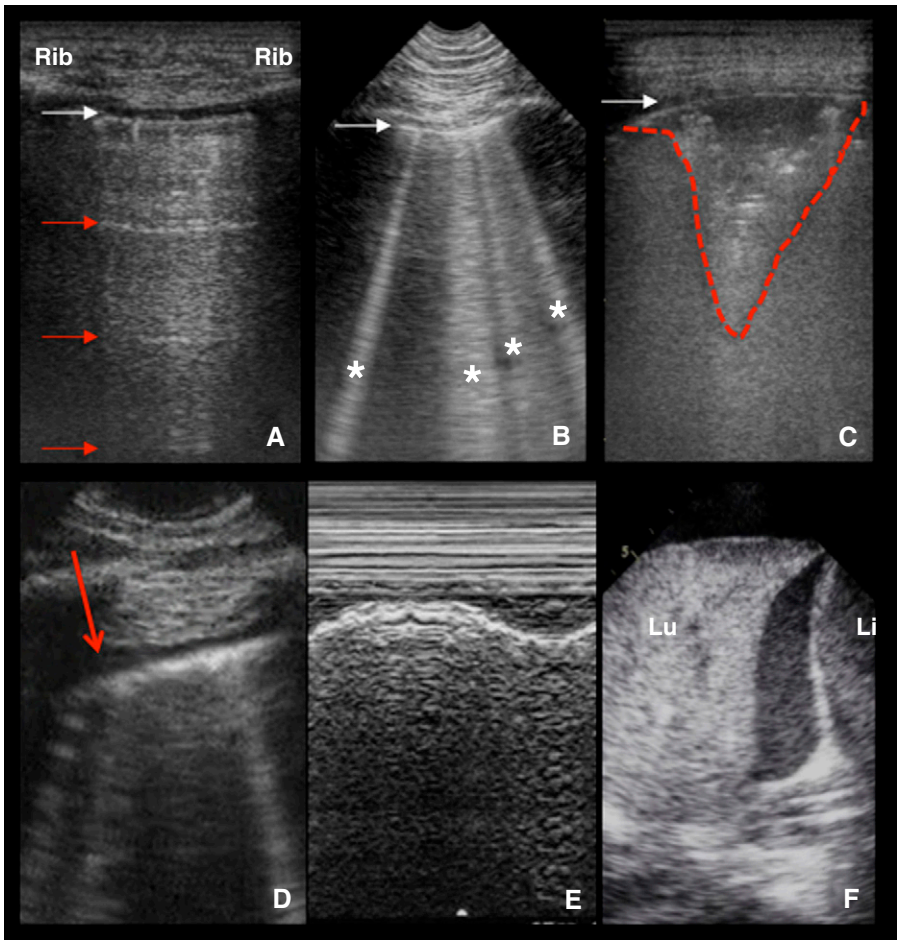

Figure 1. Basic signs of lung ultrasound. (*A*) The pleural line (white arrow) is identified between the ribs (bat sign); horizontal reverberation artifacts (A-lines, red arrow) at a regular distance indicate a high gas–volume ratio below the parietal pleura (longitudinal scan, linear probe). (*B*) B-lines (asterisks) are vertical artifacts deriving from the pleural line, moving synchronously with lung sliding, usually hyperechoic and laser shaped, usually reaching the bottom of the screen and erasing A-lines (white arrow, pleural line; longitudinal scan, microconvex probe). (*C*) Subpleural consolidation (dashed red line): an echo-poor image juxtaposed to the pleural line (white arrow) and delimited by irregular boundaries, the "shred sign" (transversal scan, linear probe). (*D*) A very small pleural effusion is visualized as a hypoechoic space between the parietal and visceral pleura (red arrow; longitudinal scan, microconvex probe). (*E*) M-mode of the same scan confirms the presence of the pleural effusion, showing the lung freely floating in it ("sinusoid sign"). (*F*) Tissue-like pattern identifies lobar consolidation, surrounded by pleural effusion (Li = liver; Lu = lung; longitudinal scan, phased-array probe).

Artifacts

Almost all acute respiratory disorders involve the pleura and are therefore accessible to lung ultrasound, which is a surface imaging technique. The lung ultrasound artifacts come from the pleura, and therefore the pleural line must be clearly detected to avoid mistakes. In adults it is located 0.5 cm below the rib line (bat sign) and always corresponds to the parietal pleura, whereas the visceral pleura can be present or not (Figure 1A).

The A-lines are horizontal hyperechoic artifacts, being repetition of the pleural line due to ultrasound reverberation between the pleura and the probe. The presence of A-lines indicates a high gas–volume ratio below the parietal pleura (Figure 1A and Video E1) (17, 18) and thus can be associated with normal lung, hyperinflation, or pneumothorax. Other ultrasound signs allow distinguishing these conditions.

The movement of the pleural line synchronous with tidal ventilation is called lung sliding and indicates that the parietal and visceral pleura are apposed, the latter sliding beneath the former (7). M-mode allows a more precise analysis of lung sliding and shows the "seashore sign" (Figure 2A). If lung sliding is absent, a "lung pulse" can often be visualized in bidimensional ultrasound and M-mode (Figure 2B): the visceral pleura only moves with the transmitted cardiac activity and not with tidal ventilation (19). Anterior lung sliding and lung pulse rule out pneumothorax and provide information about regional tidal ventilation (7, 19); the absence of lung sliding/lung pulse is visualized in M-mode as the "stratosphere sign" (Figure 2C). The lung point is the alternation of normal and abolished lung sliding with exclusive A-lines and is specific for pneumothorax: it corresponds to the point where the collapsed lung comes in touch with the parietal wall at each inspiration (Figure 2D and Video E2) (20).

The B-lines (Figure 1B) (17) are comet-tail artifacts always arising from the pleural line, moving in concert with lung sliding. They are usually well defined, long, extending to the bottom of the screen, erasing A-lines, and hyperechoic. More

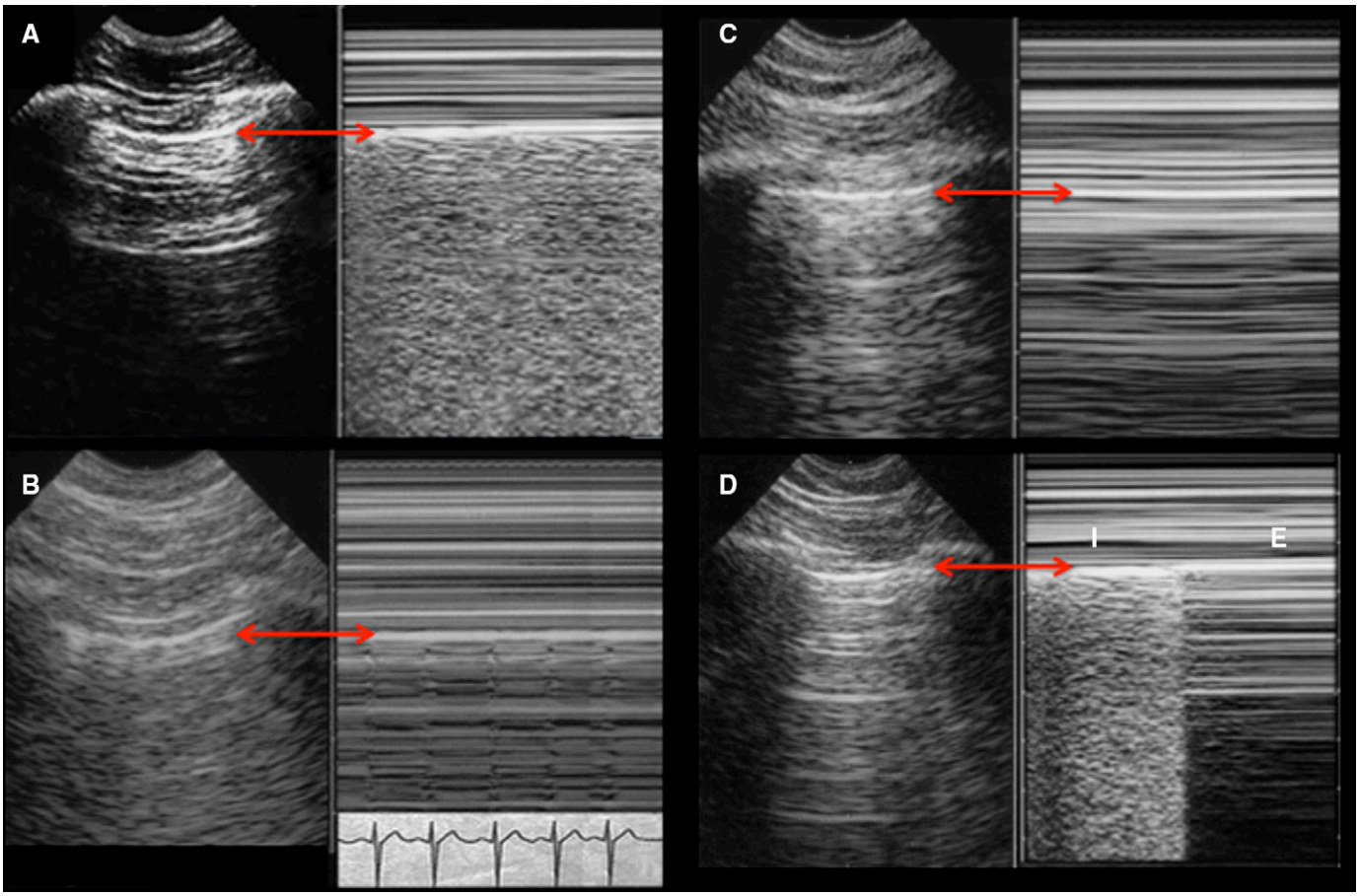

Figure 2. Basic signs of lung ultrasound in M-mode with corresponding two-dimensional images in longitudinal scan with microconvex probe; red arrows indicate the pleural line. (*A*) M-mode demonstrates normal sliding: above the pleural line; superficial tissues do not move away or toward the probe and are represented as straight lines. The pattern below the pleura is an artifact deriving from it: if the visceral pleura slides, it generates a sandy pattern ("seashore sign"). (*B*) If the visceral pleura does not slide but only beats synchronously with the heart, a different M-mode pattern is visualized (lung pulse). (*C*) A pneumothorax is suspected when no lung sliding is visualized, as confirmed by straight lines both above and below the pleural line ("stratosphere sign"). (*D*) Pneumothorax is confirmed by the presence of the lung point, visualized in M-mode as the alternation of "seashore" and "stratosphere" signs, at the location where the collapsed lung comes in touch with the parietal pleura during inspiration (E = expiration; I = inspiration).

than two B-lines per scan make a B-pattern (13), historically labeled "lung rockets," which is compatible with interstitial syndrome. Three or four B-lines correlate with thickened subpleural interlobular septa; five or more correlate with ground-glass areas and indicate severe interstitial syndrome (8).

Real Images

Fluid pleural effusion is usually a hypo- or anechoic area bounded by parietal and visceral pleurae and rib shadows (Figures 1D and 3D–3F) (21, 22). M-mode of the effusion shows the "sinusoid sign" (Figure 1E), a floating motion of the lung within the effusion in the case of low fluid viscosity (22).

Lung consolidation is either non-translobar, giving small subpleural echo-poor images with deep irregular boundaries called "shred sign" (Figure 1C and Video E3), or translobar, giving a tissue-like pattern (Figures 1F and 3A–3C) and an image shaped like an anatomical lung (23, 24). The air bronchogram is visualized as hyperechoic intraparenchymal images; it is dynamic when moving synchronous with tidal ventilation (25). Its shape can be punctiform or linear/arborescent, with different clinical interpretations (Figures 3A–3C and Videos E4–E6) (26, 27).

A Diagnostic Tool for the Acutely Ill Patient

As for other imaging techniques, lung ultrasound signs are not specific for a diagnosis *per se*. However, clinically driven lung ultrasound protocols with focused assessment allow, in particular settings and clinical conditions, to rule in or out quickly and accurately several diagnoses.

Assessment of Acute Respiratory Failure

In the BLUE protocol, lung ultrasound signs are associated to build up different profiles to be applied in patients presenting to the emergency department with dyspnea (4). Anterior diffuse lung sliding with predominant A-lines makes the A-profile. The A-profile with normal posterior fields corresponds to normal parenchyma and orients to nonparenchymal diseases (severe asthma, acute decompensation of chronic obstructive pulmonary disease [COPD]); if

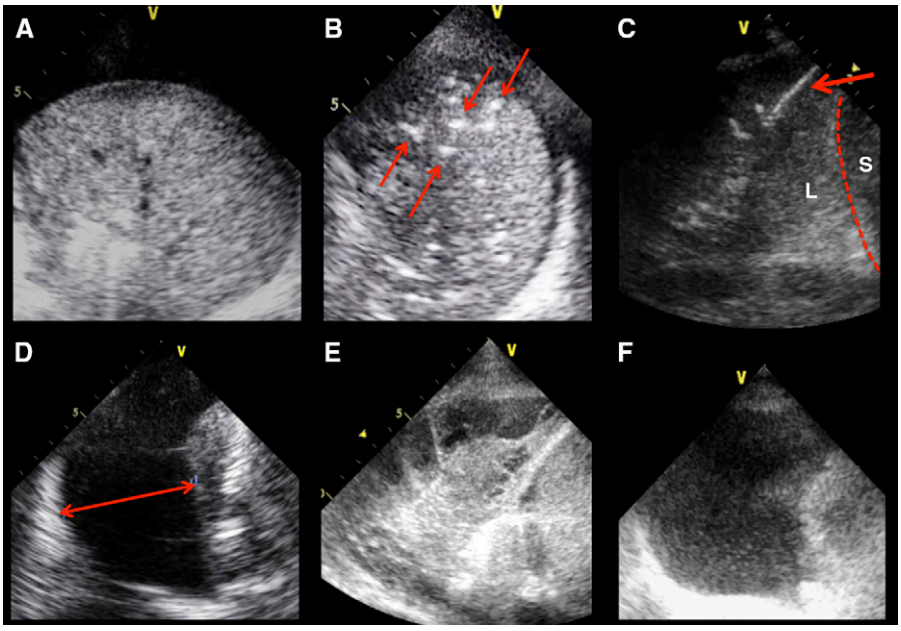

Figure 3. (*A–C*) Lobar consolidations are visualized as a tissue-like pattern; the air bronchograms are visualized as hyperechoic signs within consolidation and provide additional information on consolidation etiology. (*A*) The consolidated lung is visualized in transversal scan. It is homogeneously gray: air bronchogram is absent, which means airway is not clearly patent. Disobstructive fiber bronchoscopy may be indicated; no final conclusions on consolidation etiology can be drawn. (*B*) Multiple white spots (red arrows) are visualized within the consolidated lung in transversal scan and move synchronously with tidal ventilation: dynamic air bronchogram rules out obstructive atelectasis. (*C*) A dynamic linear/arborescent air bronchogram is specific for community-acquired and ventilator-associated pneumonia (longitudinal scan; dashed red line, diaphragm; L = lung; S = spleen). (*D–F*) Ultrasound features of pleural effusions. (*D*) Pleural effusion is here visualized in transversal scan as an anechoic space between the lung (on the right) and the posterior wall of the chest (on the left); transversal scan allows the measurement of the maximal interpleural distance (red arrow) and the quantification of the fluid collection, providing information about adequacy of chest drainage. Its homogeneous anechoic pattern orients to transudate; the lung appears partially consolidated. (*E*) Septa and adherences are visualized within the pleural effusion in transversal scan: a phlogistic etiology is suggested, and septa discourage percutaneous chest drainage. (*F*) A massive echoic pleural effusion is visualized in transversal scan between a collapsed lung (on the right) and the posterior wall of the chest (on the left); the nonhomogeneous pattern orients to exudate or blood (depending on clinical context); chest drainage is indicated.

associated with ultrasound-detected deep venous thrombosis (DVT), it strongly suggests pulmonary embolism. In a successive study, a combination of A-lines, DVT, and subpleural consolidations (corresponding to pulmonary infarctions) allowed the diagnosis of pulmonary embolism with 90% sensitivity and 86% specificity in the emergency department (28).

The A-profile with lobar consolidation in dependent lung regions is associated with pneumonia or the acute respiratory distress syndrome (ARDS) (4). The presence of A-lines without lung sliding, lung pulse, and any B-line strongly suggests pneumothorax, with high sensitivity and moderate context-dependent specificity; the lung point confirms pneumothorax with 100% specificity (4, 20, 29).

The B-profile is defined by an anterior, bilateral, symmetrical B-pattern associated with lung sliding. It may help to distinguish cardiogenic pulmonary edema from acute COPD decompensation and other diseases in the emergency department (4, 9). It is important to emphasize that a single region with a B-pattern does not indicate cardiogenic edema (30). B-pattern distribution helps in differential diagnosis (31): a monolateral B-pattern orients toward pneumonia; if bilateral (i.e., at least two regions per side) it points to cardiogenic pulmonary edema when homogeneous or to ARDS when nonhomogeneous. Assessment of this bilateral and homogeneous B-pattern is now recommended to evaluate and grade pulmonary edema during heart failure (32, 33). Additional ultrasound signs help distinguish ARDS and cardiogenic edema: patients with ARDS have nonhomogeneous lung disease combining normal areas with A-lines (spared areas), B-pattern, and subpleural and translobar consolidations, with reduced or abolished lung sliding and irregular and thickened pleural line (Videos E3 and E7 and Figure E2) (34).

In a different clinical context, patients with a known diffuse parenchymal lung disease (pulmonary fibrosis, sarcoidosis, lymphangitic carcinomatosis, etc.) also had a lung ultrasound pattern characterized by diffuse B-lines with irregular and thickened pleura when compared with the healthy population (35).

The C-profile corresponds in the BLUE protocol to anterior lung consolidations and correlates with pneumonia or ARDS (4). An ultrasound-aided definition of ARDS has also been proposed for the diagnosis in resource-limited settings: in the Kigali modification of the Berlin definition (36), bilateral infiltrates at chest X-ray are replaced by bilateral B-pattern and/or consolidation at lung ultrasound (37).

An ultrasound-based approach can save time in the assessment of dyspnea, but it needs to be integrated with a standard clinical approach to optimize diagnostic accuracy (38).

Finally, a recent single-blind randomized controlled trial showed that a cardiac, lung, and vein ultrasound protocol in patients with acute respiratory failure in the emergency department improves early accurate diagnosis, adequate treatment, and better use of advanced diagnostic tests (39).

A comprehensive flowchart for the assessment of acute respiratory failure on the basis of ultrasound findings is proposed in Figure 4.

Assessment of Circulatory Failure and Cardiac Arrest

As hypothesized by several authors (40–42) and demonstrated by a prospective observational study (3), an early multiorgan point-of-care ultrasound evaluation allows reaching almost perfect concordance with a final diagnosis of undifferentiated hypotension in the emergency ward. A combined ultrasound assessment of the right ventricle, the inferior vena cava, and the lung can rapidly rule out causes of

Table 1. Lung Ultrasound Signs, Pattern, and Clinical Interpretation

Signs	Description	Ultrasound Interpretation and Associated Patterns	Clinical Conditions and Applications	Figures Videos
Pleural line				
Bat sign	The pleural line is visualized as a horizontal hyperechoic line located in adults 0.5 cm below the rib lines in longitudinal scan in 2D	Correct identification of the pleura within the intercostal space (13)	Particularly useful in clinical conditions potentially compromising the visualization of the pleura (i.e., subcutaneous emphysema, morbid obesity)	Figure 1A, Video E1
Lung sliding	Movement of the pleural line synchronous with tidal ventilation visualized in 2D	Parietal and visceral pleura are in touch and regional ventilation is present Reduced sliding Absent sliding	Rules out pneumothorax (sensitivity, 95.3%; specificity, 91.1%; negative predictive value, 100%) (7) Suggests reduced regional ventilation (hyperinflation [78], emphysematous bullae) Suggests absent regional ventilation (78) Suggests pneumothorax with context-dependent accuracy (trauma patients: sensitivity, 98.1%; specificity, 99.2%) (70)	Video E1
Seashore sign	Straight lines above the pleural line and sandy pattern below the pleural line visualized in M-mode	Confirms the movement of the pleural line synchronous with tidal ventilation, with higher frame rate (4)	Helpful in clinical conditions where sliding is reduced or poorly visible (19)	Figure 2A
Lung pulse	Movement of the pleural line synchronous with heartbeats in absence of lung sliding (in 2D or M-mode)	Parietal and visceral pleura are in touch but regional ventilation is impaired	Confirms absence of regional ventilation (obstructed airways, hyperinflation, pleural adherence or bullae) with sensitivity 93.0%, specificity 100% (19) Rules out pneumothorax (19)	Figure 2B
Stratosphere sign	Straight horizontal lines above and beneath the pleural line in M-mode	Absence of pleural line movement either synchronous with tidal ventilation or with heartbeats. Parietal and visceral pleura may not be in touch (19)	Suggest pneumothorax with context-dependent accuracy (trauma patients: sensitivity, 98.1%; specificity, 99.2%) (70) May be due to high PEEP level (78)	Figure 2C
Lung point	Alternation of normal and abolished sliding during tidal ventilation in 2D; alternation of seashore and stratosphere sign in M-mode	Contact point between the collapsed lung and the pneumothorax air collection Its position can be mapped on the thorax Is absent when the lung is completely collapsed	Confirms pneumothorax (sensitivity, 66.0%; specificity, 100%) (20) Allows semiquantification of lung collapse: larger than 30% if below midaxillary line (sensitivity, 90.9%; specificity, 81.3%) (29)	Figure 2D, Video E2
Artifacts				
A-lines	Reverberation artifacts visualized as horizontal hyperechoic lines below the pleural line and repeated at a constant distance equal to the distance between pleural line and probe surface—visualized in 2D	High gas–volume ratio below the parietal pleura (18) A profile: A-lines with maximum 2 B-lines and lung sliding in anterior fields (4)	Corresponds to normal aeration (strong correlation with regional tissue density measured by quantitative CT scan; r_S = 0.79) (18) Rules out pneumothorax (sensitivity, 95.3%; specificity, 91.1%; negative predictive value, 100%) (7)	Figure 1A, Video E1

(Continued)

Table 1. (*Continued*)

Signs	Description	Ultrasound Interpretation and Associated Patterns	Clinical Conditions and Applications	Figures Videos
			Allows distinguishing COPD exacerbation from cardiogenic edema (sensitivity, 100%; specificity, 92.0%) (9)	
		A-lines with no lung sliding but lung pulse	Confirm absence of regional ventilation (obstructed airways, hyperinflation, pleural adherence, or bullae) with sensitivity 93.0%, specificity 100% (19) Rule out pneumothorax (19)	
		A-lines with no lung sliding and no lung pulse	Suggest absent regional ventilation (78) Suggest pneumothorax with context-dependent accuracy (trauma patients: sensitivity, 98.1%; specificity, 99.2%) (70)	
B-lines	Vertical hyperechoic comet-tail artifacts deriving from the pleural line, moving synchronously with it, usually reaching the bottom of the screen in 2D, laser-shaped, erasing the A-lines	A maximum of 2 B-lines per scan can be visualized in healthy lung	Normal lung (4, 18)	Video E1
		They originate from the visceral pleura	Rule out pneumothorax (sensitivity, 100%; specificity, 60.0%; negative predictive value, 100%) (10)	
		Increased B-lines indicate an increased density of the examined area	Air–tissue ratio is impaired; lung density is increased (strong association with tissue density measured by CT scan; R^2 = 0.62–0.78) (18)	
		B-pattern ("lung rockets"): ⩾3 B-lines per scan are visualized	Indicates interstitial syndrome (17) Allows differential diagnosis between COPD exacerbation and cardiogenic edema (sensitivity, 100%; specificity, 92.0%) (9)	Figure 1B
		B-line distribution allows distinguishing specific diseases (4, 31):		
		Focal B-pattern	Depending on the clinical context, it may correspond to pneumonia, atelectasis, lung contusion, pulmonary embolism, pleural disease, or neoplasia (4, 31)	
		Diffuse B-pattern (at least 2 regions per hemithorax):		
		Homogeneous distribution, regular thin pleura, normal sliding, and eventual bilateral pleural effusion	Orients to cardiogenic edema (34)	
		Nonhomogeneous distribution, irregular thickened pleura, subpleural and posterior consolidations	Orients to ARDS (34)	Figure E2
		Homogeneous distribution, irregular thickened pleura	Is present in 84.9–100% of cases in diffuse parenchymal lung diseases (fibrosis, sarcoidosis, silicosis, etc.) (35)	Video E7
		Number and type of B-lines allows quantification of lung aeration by the computation of the lung ultrasound score:	Predicts ARDS mortality (AUC, 0.846) (53) and weaning failure (AUC, 0.860) (16)	Figure E2
		Substantial agreement between regional lung ultrasound score and quantitative CT classification (k = 0.7) (18)	Allows monitoring aeration in patients receiving ECMO (54) and fluid resuscitation in ARDS (43)	

(*Continued*)

Table 1. (*Continued*)

Signs	Description	Ultrasound Interpretation and Associated Patterns	Clinical Conditions and Applications	Figures Videos
		Strong association between global lung ultrasound score and tissue density measured by CT scan (R^2 = 0.62–0.78) (18)	Lung ultrasound reaeration score allows monitoring of VAP response to antibiotics and PEEP-induced recruitment as measured by PV curve (correlation with CT: r = 0.85 [14] and r = 0.88 [15], respectively)	
		Strong correlation between global lung ultrasound score and EVLW measured by PiCCO (r^2 = 0.906) (53)	Lung ultrasound score variations do not correlate with PEEP-induced recruitment as measured by quantitative CT (R^2 = 0.01) (18)	
			Normal anterior fields allow distinguishing pronation responders (sensitivity, 58%; specificity, 100%; positive predictive value, 100%) (63)	
Real images				
Pleural effusion				
Interpleural hypo-/anechoic space	Dependent and usually echo-free zone acting as an acoustic window between the pleura	Fluid collection (21, 22)		Figures 3D–3F, Video E5
		Interpleural distance can be measured	Allows quantification of pleural effusion (correlation with drained pleural effusion volume, R^2 = 0.51–0.84) (68, 69)	Figure 3D
		Echotexture can be homogeneous, heterogeneous, or loculated	Allows etiologic diagnosis of the effusion (21)	Figures 3D–3F
			Guide the chest drainage (success rate, 97%) (21, 22)	
Sinusoid sign	Sinusoid aspect of visceral pleura movement within the effusion in M-mode	Confirms free fluid collection (22)	Allows distinction of echo-poor regions (free effusion, focal collection) (22)	Figure 1E
Consolidations				
Shred sign	Subpleural echo-poor images delimited by irregular borders in 2D	Small juxtapleural consolidation	Present in 36.6% of cases in diffuse parenchymal lung diseases (fibrosis, sarcoidosis, interstitial pneumonia, silicosis, etc.) (35)	Figure 1C
			May correspond to pulmonary subpleural infarcts in pulmonary embolism (alone: sensitivity, 60.9%; specificity, 95.9%; combined with vascular and cardiac ultrasound: sensitivity, 90.0%; specificity, 86.2%) (28)	Video E3
			Supports diagnosis of ventilator-associated pneumonia (alone: sensitivity, 81.0%; specificity, 41.0%; combined in the VPLUS $\geq$ 2: sensitivity, 71.0%; specificity, 69.0%) (27)	

(Continued)

Table 1. (*Continued*)

Signs	Description	Ultrasound Interpretation and Associated Patterns	Clinical Conditions and Applications	Figures Videos
Tissue-like pattern	Homogeneous texture of a lobe, similar to abdominal parenchyma in 2D	Corresponds to complete loss of aeration; a real image is visualized and the lung appears as an anatomical lung	Confirms the diagnosis of community-acquired pneumonia (sensitivity, 93.4–99%; specificity, 95–97.7%) (26, 73)	Figures 1F, 3A–3C, Videos E4–E6
Air bronchogram	Hyperechoic intraparenchymal images visualized within a tissue-like pattern in 2D	It corresponds to air trapped within the consolidation		
		If absent	Corresponds to complete air reabsorption and potentially not patent airway	Figure 3A, Video E4
		If static	Corresponds to potentially not patent airway, incomplete air reabsorption Present in 40–90% of pneumonia (25, 72)	
		If dynamic	Corresponds to patent airways: rules out atelectasis (sensitivity, 64.0%; specificity, 94.0%) (25) Is present in 86.7–97.0% of pneumonia (26, 73)	
		Linear/arborescent	Supports the diagnosis of ventilator-associated pneumonia (alone: sensitivity, 44.0%; specificity, 81.0%; combined in the VPLUS $\geq$ 2: sensitivity, 71.0%; specificity, 69.0%) (27)	Figure 3C, Video E6
		Punctiform	Is not specific for a diagnosis (27)	Figure 3B, Video E5

Definition of abbreviations: 2D = bidimensional ultrasound; ARDS = acute respiratory distress syndrome; AUC = area under the curve; COPD = chronic obstructive pulmonary disease; CT = computed tomography; ECMO = extracorporeal membrane oxygenation; EVLW = extravascular lung water; PEEP = positive end-expiratory pressure; PiCCO = pulse-contour continuous cardiac output; PV curve = pressure–volume curve; VAP = ventilator-associated pneumonia; VPLUS = ventilator-associated pneumonia lung ultrasound score.

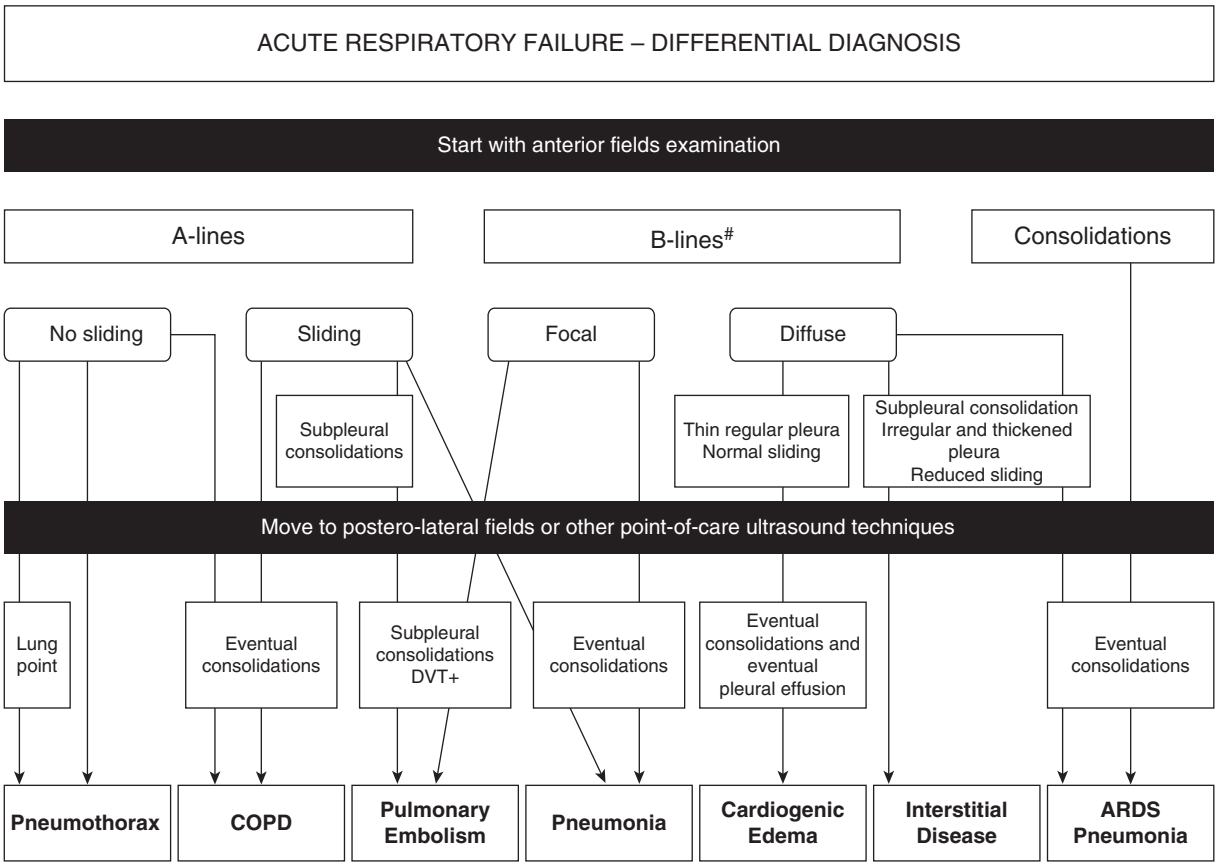

Figure 4. A proposal for a systematic diagnostic approach to acute respiratory failure based on literature findings (ARDS = acute respiratory distress syndrome; COPD = chronic pulmonary obstructive disease; DVT = deep venous thrombosis). #At least three B-lines per scan.

obstructive shock, such as substantial pericardial effusion, acute cor pulmonale, or pneumothorax. Left cardiogenic shock can be ruled in or out depending on the presence or absence of a diffuse homogeneous B-pattern. Among the remaining causes of hemodynamic instability, hypovolemic shock is expected to improve after fluid therapy, whereas distributive shock has a more variable and transient response. As recently demonstrated, the change from A-lines to B-pattern under fluid therapy early identifies lung extravascular leakage in patients with ARDS with septic shock and indicates that fluid therapy should be discontinued (43).

Accordingly, lung ultrasound can integrate and optimize an ultrasound-aided approach to the patient with sepsis (44).

Echocardiography identifies some of the causes of cardiac arrest (45) and is now recommended (33). The addition of lung, femoral vein, and abdomen ultrasound to rule out pneumothorax, DVT, and free fluid in the abdomen in cardiac arrest has been proposed (41, 46–48). To date, a single prospective application was performed, combining the evaluation of lung sliding to focused echocardiography (5).

A Monitoring Tool: Lung Aeration Assessment and Clinical Applications

The number and type of ultrasound artifacts visualized in an intercostal space vary in function of the loss of aeration of the underlying lung regions (8). As shown *in vitro* (49) and *in vivo* (50), progressive homogeneous loss of aeration determines the switch from A-lines to a B-pattern, with a progressively increasing number of B-lines that coalesce more and more. Complete loss of aeration corresponds to a tissue-like pattern.

Attempts to semiquantify loss of aeration have led to different lung ultrasound rating systems (14–16, 51, 52). The one most frequently used in the ICU distinguishes four steps of progressive loss of aeration (14–16), each corresponding to a score: A-lines or two or fewer B-lines (normal aeration, score 0), three or more well-spaced B-lines (moderate loss of aeration, score 1), coalescent B-lines (severe loss of aeration, score 2), tissue-like pattern (complete loss of aeration, score 3; Figure 5). This score is computed in six regions per hemithorax: sternum, anterior, and posterior axillary lines identify anterior, lateral, and posterior areas, each divided into superior and inferior fields (Figure E1A). The global lung ultrasound score corresponds to the sum of each region's score and ranges from 0 (all regions are well aerated) to 36 (all regions are consolidated). In patients with ARDS, the regional lung ultrasound score is strongly correlated with tissue density assessed with quantitative computed tomography (CT), with each step increase of the score from 0 to 3 being associated with a significant gain of density (18). Moreover, the global lung ultrasound

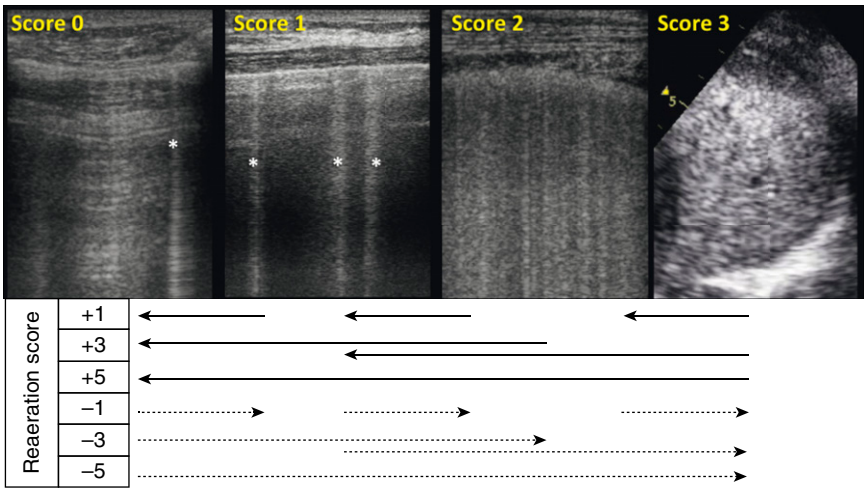

Figure 5. Semiquantification of lung aeration (transversal scans). The aeration score identifies four progressive steps of aeration (score 0: A-lines or two or fewer well-spaced B-lines; score 1: three or more well-spaced B-lines; score 2: coalescent B-lines; score 3: tissue-like pattern). It is computed in 12 standard thoracic regions. Reaeration score may be computed in the same regions to assess lung reaeration in ventilator-associated pneumonia after antibiotic treatment and in acute respiratory distress syndrome after positive end-expiratory pressure titration. Recent advances suggest to distinguish score 1 and score 2 on the basis of percentage of pleura showing B-lines or subpleural consolidations (less or greater than 50%). Asterisks indicate well-spaced B-lines.

score directly correlates both with extravascular lung water assessed by transpulmonary thermodilution (53) and with overall lung tissue density assessed by quantitative CT imaging (18).

This score has been successfully used in different clinical contexts. After a successful spontaneous breathing trial, a score higher than 17 is highly predictive of postextubation distress, whereas when lower than 13 it is highly predictive of successful weaning (16). An increase in lung ultrasound score is an early warning about the deleterious side effects of fluid resuscitation in patients with sepsis and may guide physicians in fluid administration (43).

Daily lung ultrasound scores have been monitored in patients with ARDS on venovenous extracorporeal membrane oxygenation, thus replacing chest X-ray, which is poorly informative in such severely affected lungs (54). A reaeration score on the basis of the same four patterns can be computed observing the regional changes before and after treatments aimed at improving lung aeration, as described in Figure 5; it has been successfully applied to rate antibiotic-induced reaeration in ventilator-associated pneumonia (VAP) and the increase in lung volume induced by positive end-expiratory pressure (PEEP) in patients with ARDS (14, 15).

Recent advances suggest that for nonhomogeneous diseases, such as ARDS, lung contusion, and VAP, the switch from moderate (score 1) to severe (score 2) loss of aeration might be more appropriately identified based on the percentage of the pleural line showing artifacts (55). Moreover, a weakness of the current lung ultrasound score is that complete loss of aeration (score 3) is attributed to a lung region whenever a tissue-like pattern is observed, independently of its dimension. This may lead to overestimation of loss of aeration when this pattern involves a small portion of the visualized lung region. To further improve the accuracy of ultrasound assessment of lung aeration, recent findings suggest that a score of 3 should be attributed only to regions where a tissue-like pattern is largely predominant (18).

Finally, longitudinal scan—allowing the visualization of the bat sign—is mandatory to correctly identify the pleura within the intercostal space. However, the length of visualized pleura is highly variable among different patients and in the same patient among different intercostal spaces, thus limiting reliability of a score based on number of artifacts per scan (55). Transversal scan—aligned with the intercostal space—visualized significantly wider and more constant pleural length. Thus, the transversal approach may be preferred when lung ultrasound is performed with the specific aim of a quantitative assessment of lung aeration (18, 55).

Lung Ultrasound–guided Mechanical Ventilation

Lung ultrasound was proposed as an imaging tool to guide and monitor mechanical ventilation (56, 57). First, it may help airway management: visualizing the orotracheal tube beside the trachea, it identifies esophageal intubation and, by visualizing bilateral sliding, it confirms tracheal intubation and excludes selective bronchial positioning (58).

Ultrasound can be used to guide the setting of mechanical ventilation as well. Reaeration during a recruitment maneuver can be directly and real-time visualized (59). In general, patients with diffuse loss of aeration at ultrasound examination (i.e., also affecting anterior fields) may be PEEP responders, whereas those with focal loss of aeration (i.e., posterior consolidation with normal anterior fields) are more prone to overdistension of the normal parenchyma (15), as previously indicated by CT studies (60). Changes in lung ultrasound score correlated with PEEP-induced increases of end-expiratory lung volume and were therefore proposed for bedside assessment of lung recruitment (15). However, this volume increase does not correspond to the reinflation of previously collapsed lung tissue (i.e., lung recruitment), as most of the gas enters already inflated lung regions (61). Accordingly, lung ultrasound score parallels lung tissue density and aeration in patients with ARDS, but changes of lung ultrasound score are not related to the amount of recruitable lung tissue (18). Whether PEEP-induced changes in size of tissue-like areas could be used to assess lung recruitment at the bedside, although reasonable, remains to be demonstrated (62).

Patients classified as PEEP nonresponders may successfully respond to prone positioning (63). In patients with focal loss of aeration and a normal anterior lung ultrasound pattern, consolidated posterior regions did, in fact, show greater reaeration with prone positioning than in patients with more diffuse disease (64). Moreover, the amount of reaeration of posterior lung regions assessed by

ultrasound after 3 hours of prone position was associated with a positive clinical response, defined as a partial pressure of arterial oxygen to fraction of inspired oxygen higher than 300 mm Hg after 7 days of treatment (Figure E1B) (65).

As already stated, the lung ultrasound score can help distinguish patients at high and low risk of postextubation distress (16). A score 2 pattern seems to best identify the failing patients (66). The lung ultrasound score predicts extubation failure probably because decreased pulmonary aeration is a final common pathway of patients failing extubation for different reasons. The combination of lung ultrasound and other ultrasound techniques in the assessment of the patients to be weaned has been suggested not only to identify the frailest patients early but also to understand the underlying mechanism, being the main causes of weaning failure detectable with ultrasound (i.e., unsolved lung disease, diaphragm dysfunction, and cardiac failure) (66, 67).

Detection and Management of Respiratory Complications in Mechanically Ventilated Patients

Lung ultrasound, thanks to its ready availability at the bedside, could become a key tool for the early diagnosis of the most common complications of mechanical ventilation, such as pleural effusion, alveolar consolidation related to atelectasis or VAP, and pneumothorax (56, 57).

Pleural effusion appears as a dependent, usually echo-free, zone acting as an acoustic window (Figures 3D–3F) (21, 22). Inside the pleural effusion, the lung can be seen as a bright lung line if it remains aerated or as a floating consolidation if not. Pleural effusion can be easily distinguished from perisplenic or perihepatic fluid collections by the visualization of the diaphragm in longitudinal scan. Lung ultrasound also allows accurate and clinically useful estimates of the volume of effusion (68): in supine position, in transversal scan, an interpleural distance of 5 cm or more at the lung base is highly predictive of pleural effusion of 500 ml or more. A linear relationship has also been identified, each centimeter of interpleural distance corresponding to 200 ml of fluid (69). Transudates are always anechoic and homogeneous, whereas exudates may appear echoic, heterogeneous, and loculated (Figures 3D–3F) (21). Lung ultrasound is also a valid tool to guide effusion drainage and monitor its effectiveness (21, 22).

The interposition of gas between the visceral and parietal pleura is marked by the absence of lung sliding, B-lines, and lung pulse (7, 10, 19). Diagnosis of pneumothorax is confirmed by the visualization of a lung point in a more lateral part of the chest wall (20). This corresponds to the limit of the pneumothorax (Figure 2D and Video E2) and can be used to measure its extension (29): a lung point beneath the midaxillary line in a presumed free collection indicates a collapse of at least 30% of the parenchyma. However, in a completely collapsed lung, no lung point can be visualized. Lung ultrasound performs better than chest X-ray for diagnosing pneumothorax, particularly in trauma patients (70, 71).

In the emergency room, lung ultrasound is a valid alternative for early diagnosis of pneumonia in adults (4, 26, 38, 39, 72, 73). Consolidations have 93% sensitivity and 98% specificity for the diagnosis of community-acquired pneumonia (72). In ICU patients, intricate causes of loss of aeration may give rise to B-pattern and consolidations. Consequently, in these patients a tissue-like pattern is not sufficient for the diagnosis (27); instead, the presence of a dynamic linear/arborescent air bronchogram within a consolidation seems to be a specific sign of VAP. A clinical ultrasound score can be easily computed at the bedside for early VAP diagnosis (27).

Typically, reabsorption atelectasis appears as consolidated parenchyma with a reduced lung volume; the air bronchogram is either static (initial phase) or completely absent (complete reabsorption of air in small airways; Figure 3A and Video E4). If the air bronchogram is dynamic, obstructive atelectasis is ruled out (Videos E5 and E6) (25). No or static air bronchogram suggests nonpatent airway and may be an indication for disobstructive fiber bronchoscopy; a dynamic air bronchogram corresponds to patent airways, and fiber bronchoscopy may also be indicated to obtain a distal microbiological sample (27).

The vascularization of a lung consolidation can be visualized by color Doppler. A well-perfused lung region with complete loss of aeration corresponds to intrapulmonary shunt, thus suggesting a significant contribution of the consolidation to hypoxemia. However, color Doppler assessment of lung perfusion is only qualitative; a quantitative assessment may be useful in the future to quantify the intrapulmonary shunt and monitor the response to treatments (74).

Limitations of Lung Ultrasound

Like other ultrasound techniques, lung ultrasound is operator-dependent and requires training for image acquisition and interpretation. Concerning image acquisition for lung aeration assessment, interobserver agreement was almost perfect (18); in image interpretation, interoperator agreement was strong or almost perfect, depending on the scoring system adopted (55). Simple findings can be easily acquired with a short training: anesthesia residents were able to rule out pneumothorax after 5 minutes of on-line training (75), and pleural effusions were easily detected by ICU residents after a few hours of theoretical and hands-on work (76). For more advanced skills, such as lung ultrasound score computation, a longer training with 25 supervised examinations allowed acceptable concordance between trainees and experts to be reached (77). Lung ultrasound is an additional workload for the physician; however, time required to perform an extensive examination for lung aeration assessment ranged from 8 minutes for experts to 10 minutes for trainees (77).

Lung ultrasound depends on transmission of ultrasound beams through the chest wall to the lung surface. This propagation from skin to lung can be prevented by subcutaneous emphysema or large thoracic dressings. Once the ultrasound beams are transmitted and the lung is aerated, the examination only allows analysis of the lung surface. This means that only fields immediately beneath the probe are explored, thus underlying the need for as comprehensive and systematic an examination as possible. Moreover, caution is recommended in the interpretation of lung ultrasound findings in diseases

that may have no or minimal extension to peripheral fields (i.e., deep peribronchial mass/abscess, histiocytosis, tuberculosis, aspergillosis, bronchiectasis).

Finally, no specific lung ultrasound sign has been found for the detection of lung overinflation (57).

Future Perspectives for Lung Ultrasound

As a monitoring tool, semiquantitative assessment of lung aeration has greatly developed in the last few years (14–16, 51–54). A better bedside aeration assessment awaits improvement of the current scoring system with different definitions of moderate and severe loss of aeration (55) and finer quantification of the nonaerated tissue within consolidations (18, 62). One additional potential improvement is the detection of overinflation, which is reasonably suggested by reduced sliding (57, 78); however, lung sliding has never been objectively quantified and relies on "eyeball assessment" by expert examiners.

Automation is also being examined, with a view to computing aeration automatically on the basis of the computer-assisted gray-scale analysis (79) or automatic counting of the B-lines (80).

Hand-held devices are now available. Whether they will improve ultrasound assessment of the critically ill and gradually replace stethoscopes in physicians' pockets is still unclear.

Conclusions

Lung ultrasound is a simple bedside technique with numerous potential translational applications. It may help physicians in the diagnosis of the main respiratory disorders affecting the critically ill, thus suggesting the therapeutic approach in the emergency department and ICU.

Lung ultrasound can be used to assess and monitor lung aeration in the patient with acute respiratory failure and may be a useful tool to guide mechanical ventilation and several procedures, such as recruitment maneuvers, pronation, fiber bronchoscopy, and pleural drainage.

As a consequence, lung ultrasound has generated worldwide enthusiasm among physicians involved in the treatment of critically ill patients. Many clinical applications are now suggested; the extent of their clinical impact and whether lung ultrasound should be part of the basic knowledge of all intensivists will be assessed in the future. ■

Author disclosures are available with the text of this article at www.atsjournals.org.

References

1. Zieleskiewicz L, Muller L, Lakhal K, Meresse Z, Arbelot C, Bertrand PM, *et al*.; CAR'Echo and AzuRea Collaborative Networks. Point-of-care ultrasound in intensive care units: assessment of 1073 procedures in a multicentric, prospective, observational study. *Intensive Care Med* 2015;41:1638–1647.
2. Lamperti M, Bodenham AR, Pittiruti M, Blaivas M, Augoustides JG, Elbarbary M, *et al*. International evidence-based recommendations on ultrasound-guided vascular access. *Intensive Care Med* 2012;38: 1105–1117.
3. Volpicelli G, Lamorte A, Tullio M, Cardinale L, Giraudo M, Stefanone V, *et al*. Point-of-care multiorgan ultrasonography for the evaluation of undifferentiated hypotension in the emergency department. *Intensive Care Med* 2013;39:1290–1298.
4. Lichtenstein DA, Mezière GA. Relevance of lung ultrasound in the diagnosis of acute respiratory failure: the BLUE protocol. *Chest* 2008; 134:117–125.
5. Lien WC, Hsu SH, Chong KM, Sim SS, Wu MC, Chang WT, *et al*. US-CAB protocol for ultrasonographic evaluation during cardiopulmonary resuscitation: validation and potential impact. *Resuscitation* 2018;127: 125–131.
6. Ross AM, Genton E, Holmes JH. Ultrasonic examination of the lung. *J Lab Clin Med* 1968;72:556–564.
7. Lichtenstein DA, Menu Y. A bedside ultrasound sign ruling out pneumothorax in the critically ill: lung sliding. *Chest* 1995;108: 1345–1348.
8. Lichtenstein D, Mézière G, Biderman P, Gepner A, Barré O. The comet-tail artifact: an ultrasound sign of alveolar-interstitial syndrome. *Am J Respir Crit Care Med* 1997;156:1640–1646.
9. Lichtenstein D, Mezière G. A lung ultrasound sign allowing bedside distinction between pulmonary edema and COPD: the comet-tail artifact. *Intensive Care Med* 1998;24:1331–1334.
10. Lichtenstein D, Mezière G, Biderman P, Gepner A. The comet-tail artifact: an ultrasound sign ruling out pneumothorax. *Intensive Care Med* 1999;25:383–388.
11. Xirouchaki N, Kondili E, Prinianakis G, Malliotakis P, Georgopoulos D. Impact of lung ultrasound on clinical decision making in critically ill patients. *Intensive Care Med* 2014;40:57–65.
12. Brogi E, Bignami E, Sidoti A, Shawar M, Gargani L, Vetrugno L, *et al*. Could the use of bedside lung ultrasound reduce the number of chest x-rays in the intensive care unit? *Cardiovasc Ultrasound* 2017;15:23.
13. Volpicelli G, Elbarbary M, Blaivas M, Lichtenstein DA, Mathis G, Kirkpatrick AW, *et al*.; International Liaison Committee on Lung Ultrasound (ILC-LUS) for International Consensus Conference on Lung Ultrasound (ICC-LUS). International evidence-based recommendations for point-of-care lung ultrasound. *Intensive Care Med* 2012;38:577–591.
14. Bouhemad B, Liu ZH, Arbelot C, Zhang M, Ferarri F, Le-Guen M, *et al*. Ultrasound assessment of antibiotic-induced pulmonary reaeration in ventilator-associated pneumonia. *Crit Care Med* 2010;38:84–92.
15. Bouhemad B, Brisson H, Le-Guen M, Arbelot C, Lu Q, Rouby JJ. Bedside ultrasound assessment of positive end-expiratory pressure-induced lung recruitment. *Am J Respir Crit Care Med* 2011;183:341–347.
16. Soummer A, Perbet S, Brisson H, Arbelot C, Constantin JM, Lu Q, *et al*.; Lung Ultrasound Study Group. Ultrasound assessment of lung aeration loss during a successful weaning trial predicts postextubation distress. *Crit Care Med* 2012;40:2064–2072.
17. Lichtenstein DA, Mezière GA, Lagoueyte JF, Biderman P, Goldstein I, Gepner A. A-lines and B-lines: lung ultrasound as a bedside tool for predicting pulmonary artery occlusion pressure in the critically ill. *Chest* 2009;136:1014–1020.
18. Chiumello D, Mongodi S, Algieri I, Vergani GL, Orlando A, Via G, *et al*. Assessment of lung aeration and recruitment by CT scan and ultrasound in acute respiratory distress syndrome patients. *Crit Care Med* 2018;46:1761–1768.
19. Lichtenstein DA, Lascols N, Prin S, Mezière G. The "lung pulse": an early ultrasound sign of complete atelectasis. *Intensive Care Med* 2003;29:2187–2192.
20. Lichtenstein D, Mezière G, Biderman P, Gepner A. The "lung point": an ultrasound sign specific to pneumothorax. *Intensive Care Med* 2000; 26:1434–1440.
21. Yu CJ, Yang PC, Chang DB, Luh KT. Diagnostic and therapeutic use of chest sonography: value in critically ill patients. *AJR Am J Roentgenol* 1992;159:695–701.
22. Lichtenstein D, Hulot JS, Rabiller A, Tostivint I, Mezière G. Feasibility and safety of ultrasound-aided thoracentesis in mechanically ventilated patients. *Intensive Care Med* 1999;25:955–958.
23. Yang PC, Luh KT, Chang DB, Yu CJ, Kuo SH, Wu HD. Ultrasonographic evaluation of pulmonary consolidation. *Am Rev Respir Dis* 1992;146: 757–762.
24. Lichtenstein DA, Lascols N, Mezière G, Gepner A. Ultrasound diagnosis of alveolar consolidation in the critically ill. *Intensive Care Med* 2004; 30:276–281.

25. Lichtenstein D, Mezière G, Seitz J. The dynamic air bronchogram: a lung ultrasound sign of alveolar consolidation ruling out atelectasis. *Chest* 2009;135:1421–1425.
26. Reissig A, Copetti R, Mathis G, Mempel C, Schuler A, Zechner P, *et al*. Lung ultrasound in the diagnosis and follow-up of community-acquired pneumonia: a prospective, multicenter, diagnostic accuracy study. *Chest* 2012;142:965–972.
27. Mongodi S, Via G, Girard M, Rouquette I, Misset B, Braschi A, *et al*. Lung ultrasound for early diagnosis of ventilator-associated pneumonia. *Chest* 2016;149:969–980.
28. Nazerian P, Vanni S, Volpicelli G, Gigli C, Zanobetti M, Bartolucci M, *et al*. Accuracy of point-of-care multiorgan ultrasonography for the diagnosis of pulmonary embolism. *Chest* 2014;145:950–957.
29. Volpicelli G, Boero E, Sverzellati N, Cardinale L, Busso M, Boccuzzi F, *et al*. Semi-quantification of pneumothorax volume by lung ultrasound. *Intensive Care Med* 2014;40:1460–1467.
30. Bataille B, Riu B, Ferre F, Moussot PE, Mari A, Brunel E, *et al*. Integrated use of bedside lung ultrasound and echocardiography in acute respiratory failure: a prospective observational study in ICU. *Chest* 2014;146:1586–1593.
31. Volpicelli G, Caramello V, Cardinale L, Mussa A, Bar F, Frascisco MF. Detection of sonographic B-lines in patients with normal lung or radiographic consolidations. *Med Sci Monit* 2008;14:CR122–128.
32. Gheorghiade M, Follath F, Ponikowski P, Barsuk JH, Blair JE, Cleland JG, *et al*.; European Society of Cardiology; European Society of Intensive Care Medicine. Assessing and grading congestion in acute heart failure: a scientific statement from the acute heart failure committee of the heart failure association of the European Society of Cardiology and endorsed by the European Society of Intensive Care Medicine. *Eur J Heart Fail* 2010;12:423–433.
33. Lancellotti P, Price S, Edvardsen T, Cosyns B, Neskovic AN, Dulgheru R, *et al*. The use of echocardiography in acute cardiovascular care: recommendations of the European Association of Cardiovascular Imaging and the Acute Cardiovascular Care Association. *Eur Heart J Cardiovasc Imaging* 2015;16:119–146.
34. Copetti R, Soldati G, Copetti P. Chest sonography: a useful tool to differentiate acute cardiogenic pulmonary edema from acute respiratory distress syndrome. *Cardiovasc Ultrasound* 2008;6:16.
35. Reissig A, Kroegel C. Transthoracic sonography of diffuse parenchymal lung disease: the role of comet tail artifacts. *J Ultrasound Med* 2003; 22:173–180.
36. Ranieri VM, Rubenfeld GD, Thompson BT, Ferguson ND, Caldwell E, Fan E, *et al*.; ARDS Definition Task Force. Acute respiratory distress syndrome: the Berlin Definition. *JAMA* 2012;307:2526–2533.
37. Riviello ED, Kiviri W, Twagirumugabe T, Mueller A, Banner-Goodspeed VM, Officer L, *et al*. Hospital incidence and outcomes of the acute respiratory distress syndrome using the Kigali modification of the Berlin definition. *Am J Respir Crit Care Med* 2016;193:52–59.
38. Zanobetti M, Scorpiniti M, Gigli C, Nazerian P, Vanni S, Innocenti F, *et al*. Point-of-care ultrasonography for evaluation of acute dyspnea in the ED. *Chest* 2017;151:1295–1301.
39. Laursen CB, Sloth E, Lassen AT, Christensen Rd, Lambrechtsen J, Madsen PH, *et al*. Point-of-care ultrasonography in patients admitted with respiratory symptoms: a single-blind, randomised controlled trial. *Lancet Respir Med* 2014;2:638–646.
40. Perera P, Mailhot T, Riley D, Mandavia D. The RUSH exam: Rapid Ultrasound in SHock in the evaluation of the critically ill. *Emerg Med Clin North Am* 2010;28:29–56, vii.
41. Copetti R, Copetti P, Reissig A. Clinical integrated ultrasound of the thorax including causes of shock in nontraumatic critically ill patients: a practical approach. *Ultrasound Med Biol* 2012;38:349–359.
42. Lichtenstein DA. BLUE-protocol and FALLS-protocol: two applications of lung ultrasound in the critically ill. *Chest* 2015;147:1659–1670.
43. Caltabeloti F, Monsel A, Arbelot C, Brisson H, Lu Q, Gu WJ, *et al*. Early fluid loading in acute respiratory distress syndrome with septic shock deteriorates lung aeration without impairing arterial oxygenation: a lung ultrasound observational study. *Crit Care* 2014;18:R91.
44. Coen D, Cortellaro F, Pasini S, Tombini V, Vaccaro A, Montalbetti L, *et al*. Towards a less invasive approach to the early goal-directed treatment of septic shock in the ED. *Am J Emerg Med* 2014;32: 563–568.
45. Breitkreutz R, Price S, Steiger HV, Seeger FH, Ilper H, Ackermann H, *et al*.; Emergency Ultrasound Working Group of the Johann Wolfgang Goethe-University Hospital, Frankfurt am Main. Focused echocardiographic evaluation in life support and peri-resuscitation of emergency patients: a prospective trial. *Resuscitation* 2010;81: 1527–1533.
46. Testa A, Cibinel GA, Portale G, Forte P, Giannuzzi R, Pignataro G, *et al*. The proposal of an integrated ultrasonographic approach into the ALS algorithm for cardiac arrest: the PEA protocol. *Eur Rev Med Pharmacol Sci* 2010;14:77–88.
47. Volpicelli G. Usefulness of emergency ultrasound in nontraumatic cardiac arrest. *Am J Emerg Med* 2011;29:216–223.
48. Lichtenstein DA. How can the use of lung ultrasound in cardiac arrest make ultrasound a holistic discipline: the example of the SESAME-protocol. *Med Ultrason* 2014;16:252–255.
49. Soldati G, Inchingolo R, Smargiassi A, Sher S, Nenna R, Inchingolo CD, *et al*. Ex vivo lung sonography: morphologic-ultrasound relationship. *Ultrasound Med Biol* 2012;38:1169–1179.
50. Via G, Lichtenstein D, Mojoli F, Rodi G, Neri L, Storti E, *et al*. Whole lung lavage: a unique model for ultrasound assessment of lung aeration changes. *Intensive Care Med* 2010;36:999–1007.
51. Baldi G, Gargani L, Abramo A, D'Errico L, Caramella D, Picano E, *et al*. Lung water assessment by lung ultrasonography in intensive care: a pilot study. *Intensive Care Med* 2013;39:74–84.
52. Volpicelli G, Caramello V, Cardinale L, Mussa A, Bar F, Frascisco MF. Bedside ultrasound of the lung for the monitoring of acute decompensated heart failure. *Am J Emerg Med* 2008;26:585–591.
53. Zhao Z, Jiang L, Xi X, Jiang Q, Zhu B, Wang M, *et al*. Prognostic value of extravascular lung water assessed with lung ultrasound score by chest sonography in patients with acute respiratory distress syndrome. *BMC Pulm Med* 2015;15:98.
54. Mongodi S, Pozzi M, Orlando A, Bouhemad B, Stella A, Tavazzi G, *et al*. Lung ultrasound for daily monitoring of ARDS patients on extracorporeal membrane oxygenation: preliminary experience. *Intensive Care Med* 2018;44:123–124.
55. Mongodi S, Bouhemad B, Orlando A, Stella A, Tavazzi G, Via G, *et al*. Modified lung ultrasound score for assessing and monitoring pulmonary aeration. *Ultraschall Med* 2017;38:530–537.
56. Bouhemad B, Mongodi S, Via G, Rouquette I. Ultrasound for "lung monitoring" of ventilated patients. *Anesthesiology* 2015;122:437–447.
57. Pesenti A, Musch G, Lichtenstein D, Mojoli F, Amato MBP, Cinnella G, *et al*. Imaging in acute respiratory distress syndrome. *Intensive Care Med* 2016;42:686–698.
58. Hoffmann B, Gullett JP, Hill HF, Fuller D, Westergaard MC, Hosek WT, *et al*. Bedside ultrasound of the neck confirms endotracheal tube position in emergency intubations. *Ultraschall Med* 2014;35: 451–458.
59. Tusman G, Acosta CM, Costantini M. Ultrasonography for the assessment of lung recruitment maneuvers. *Crit Ultrasound J* 2016;8:8.
60. Constantin JM, Grasso S, Chanques G, Aufort S, Futier E, Sebbane M, *et al*. Lung morphology predicts response to recruitment maneuver in patients with acute respiratory distress syndrome. *Crit Care Med* 2010;38:1108–1117.
61. Chiumello D, Marino A, Brioni M, Cigada I, Menga F, Colombo A, *et al*. Lung recruitment assessed by respiratory mechanics and computed tomography in patients with acute respiratory distress syndrome: what is the relationship? *Am J Respir Crit Care Med* 2016;193:1254–1263.
62. Gardelli G, Feletti F, Gamberini E, Bonarelli S, Nanni A, Mughetti M. Using sonography to assess lung recruitment in patients with acute respiratory distress syndrome. *Emerg Radiol* 2009;16:219–221.
63. Prat G, Guinard S, Bizien N, Nowak E, Tonnelier JM, Alavi Z, *et al*. Can lung ultrasonography predict prone positioning response in acute respiratory distress syndrome patients? *J Crit Care* 2016;32:36–41.
64. Haddam M, Zieleskiewicz L, Perbet S, Baldovini A, Guervilly C, Arbelot C, *et al*.; CAR'Echo Collaborative Network; AzuRea Collaborative Network. Lung ultrasonography for assessment of oxygenation response to prone position ventilation in ARDS. *Intensive Care Med* 2016;42:1546–1556.
65. Wang XT, Ding X, Zhang HM, Chen H, Su LX, Liu DW; Chinese Critical Ultrasound Study Group (CCUSG). Lung ultrasound can be used to predict the potential of prone positioning and assess prognosis in patients with acute respiratory distress syndrome. *Crit Care* 2016;20:385.

66. Silva S, Ait Aissa D, Cocquet P, Hoarau L, Ruiz J, Ferre F, *et al*. Combined thoracic ultrasound assessment during a successful weaning trial predicts postextubation distress. *Anesthesiology* 2017; 127:666–674.
67. Mongodi S, Via G, Bouhemad B, Storti E, Mojoli F, Braschi A. Usefulness of combined bedside lung ultrasound and echocardiography to assess weaning failure from mechanical ventilation: a suggestive case. *Crit Care Med* 2013;41:e182–e185.
68. Vignon P, Chastagner C, Berkane V, Chardac E, François B, Normand S, *et al*. Quantitative assessment of pleural effusion in critically ill patients by means of ultrasonography. *Crit Care Med* 2005;33: 1757–1763.
69. Balik M, Plasil P, Waldauf P, Pazout J, Fric M, Otahal M, *et al*. Ultrasound estimation of volume of pleural fluid in mechanically ventilated patients. *Intensive Care Med* 2006;32:318.
70. Blaivas M, Lyon M, Duggal S. A prospective comparison of supine chest radiography and bedside ultrasound for the diagnosis of traumatic pneumothorax. *Acad Emerg Med* 2005;12:844–849.
71. Soldati G, Testa A, Sher S, Pignataro G, La Sala M, Silveri NG. Occult traumatic pneumothorax: diagnostic accuracy of lung ultrasonography in the emergency department. *Chest* 2008;133: 204–211.
72. Gehmacher O, Mathis G, Kopf A, Scheier M. Ultrasound imaging of pneumonia. *Ultrasound Med Biol* 1995;21:1119–1122.
73. Cortellaro F, Colombo S, Coen D, Duca PG. Lung ultrasound is an accurate diagnostic tool for the diagnosis of pneumonia in the emergency department. *Emerg Med J* 2012;29:19–23.
74. Mongodi S, Bouhemad B, Iotti GA, Mojoli F. An ultrasonographic sign of intrapulmonary shunt. *Intensive Care Med* 2016;42:912–913.
75. Krishnan S, Kuhl T, Ahmed W, Togashi K, Ueda K. Efficacy of an online education program for ultrasound diagnosis of pneumothorax. *Anesthesiology* 2013;118:715–721.
76. Vignon P, Mücke F, Bellec F, Marin B, Croce J, Brouqui T, *et al*. Basic critical care echocardiography: validation of a curriculum dedicated to noncardiologist residents. *Crit Care Med* 2011;39:636–642.
77. Rouby JJ, Arbelot C, Gao Y, Zhang M, Lv J, An Y, *et al*.; APECHO study group. Training for Lung Ultrasound Score Measurement in Critically Ill Patients. *Am J Respir Crit Care Med* [online ahead of print] 20 Mar 2018; DOI: 10.1164/rccm.201802-0227LE.
78. Markota A, Golub J, Stožer A, Fluher J, Prosen G, Bergauer A, *et al*. Absence of lung sliding is not a reliable sign of pneumothorax in patients with high positive end-expiratory pressure. *Am J Emerg Med* 2016;34:2034–2036.
79. Corradi F, Brusasco C, Vezzani A, Santori G, Manca T, Ball L, *et al*. Computer-aided quantitative ultrasonography for detection of pulmonary edema in mechanically ventilated cardiac surgery patients. *Chest* 2016;150:640–651.
80. Anantrasirichai N, Hayes W, Allinovi M, Bull D, Achim A. Line detection as an inverse problem: application to lung ultrasound imaging. *IEEE Trans Med Imaging* 2017;36:2045–2056.